

Chemical Communications

Supporting information

A neutral diphosphene radical: synthesis, electronic structure and white phosphorus activation

Jan Haberstroh,^a Clemens Taube,^a Jannis Fidelius,^a Stephen Schulz,^a Noel Israel,^b Evgenia Dmitrieva,^b Rosa M. Gomila,^c Antonio Frontera,^c Robert Wolf,^d Kai Schwedtmann,^a Jan J. Weigand^{1*ac}

a Chair of Inorganic Molecular Chemistry, Faculty of Chemistry and Food Chemistry, Technische Universität Dresden, 01069 Dresden, Germany

b Leibniz-Institute for Solid State and Materials Research Dresden, 01069 Dresden, Germany

c Department of Chemistry, Universitat de les Illes Balears, 07122 Palma de Mallorca, Spain.

d Institute of Inorganic Chemistry, Universität Regensburg, 93040 Regensburg, Germany

e Department of Chemistry and Polymer Science, Stellenbosch University, Stellenbosch, South Africa

Contents

1	Experimental Section	3
1.1	General Remarks	3
1.2	Preparation of $(^{CL}IM^{DIPP})P-P(DIPP) 1'$	4
1.3	Preparation of $1'$ from 3	6
1.4	Further investigation of the reactivity of of $1'$	7
1.5	Preparation of $[(^{CL}IM^{DIPP})P-P(DIPP)]_2-P_4 4$	8
1.6	Preparation of 4 from 3 in a stoichiometric ratio with P_4	12
1.7	Preparation of 4 from 3 in a 1 to 1 ratio with P_4	12
1.8	Investigation of the ratio of isomers of 4	13
2	Iteration of NMR spectra.....	14
3	Electrochemical procedures and Data	17
4	DFT calculation of molecular orbitals and spin density and computational details	20
4.1	Computational methods.....	20
4.2	Discussion of the frontier orbitals and spin density	20
4.3	Mechanistic Studies.....	21
4.3	Cartesian Coordinates of the optimized radical:	23
5	Crystallography	28
5.1	General Remarks	28
5.2	Crystallographic data.....	29

1 Experimental Section

1.1 General Remarks

All manipulations were performed in a Glovebox MB Unilab or using Schlenk techniques under an atmosphere of purified nitrogen or argon, respectively. All glassware was oven-dried at 160 °C prior to use. Dry, oxygen-free solvents such as CH₂Cl₂, C₆H₅F, CH₃CN, *n*-pentane, *n*-hexane, THF, Et₂O, Toluene, Benzene (distilled from potassium or CaCH₂ (for CH₂Cl and CH₃CN)) were employed. All distilled and deuterated solvents were stored over 4 Å molecular sieves, except for CD₃CN and CH₃CN, which were stored over 3 Å molecular sieves.

Melting points were recorded on an electrothermal melting point apparatus (Büchi Switzerland, Melting point M-560) in sealed capillaries under Nitrogen atmosphere.

EPR measurements were recorded using a ca. 0.5 mM solution of **1** in dry and degassed CH₃CN in a sealed glass capillary. EPR spectra were performed using a CW X-band EMXplus spectrometer with a premiumX microwave bridge (Bruker) and a high sensitivity resonator (ER 4119 HS, Bruker). The EPR spectra were registered at 100 kHz modulation at room temperature. For the precise determination of *g*-values, an NMR teslameter (ER036TM, Bruker) was used. The simulation of the EPR spectrum was done using the SpinFit module incorporated in the Xenon software of the spectrometer.

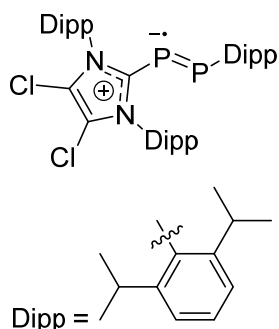
Infrared (IR) and Raman spectra were recorded at ambient temperature using a Bruker Vertex 70 instrument equipped with a RAM II module (Nd-YAG laser, 1064 nm). The Raman intensities are reported in percent relative to the most intense peak and are given in parenthesis. An ATR unit (diamond) was used for recording IR spectra. The intensities are reported relative to the most intense peak and are given in parenthesis using the following abbreviations: vw = very weak, w = weak, m = medium, s = strong, vs = very strong.

Elemental analyses were performed on a Vario MICRO cube Elemental Analyzer by Elementar Analysatorsysteme GmbH in CHNS mode.

NMR spectra were measured on a Bruker AVANCE III HD Nanobay 400 MHz Ultrashield (¹H = 400.13 MHz, ¹³C = 100.61 MHz, ¹⁹F = 376.50 MHz, ³¹P = 161.98 MHz) or Bruker AVANCE III HDX 500 MHz Ascend (¹H = 500.13 MHz, ¹³C = 125.75 MHz, ¹⁹F = 470.59 MHz, ³¹P = 202.45 MHz) and analyzed using the software Topspin v3.2 (Bruker). Chemical shifts δ are referenced to the external standards tetramethylsilane (¹H, ¹³C) trichlorofluoromethane (¹⁹F), or phosphoric acid 85 % (³¹P) and are given in ppm. Coupling constants over *n* bonds ^{*n*}*J* are given in Hz. Unless stated otherwise, all spectra were measured at 300 K. Reported numbers assigning atoms in the ¹³C spectra were deduced from 2D correlation experiments (HSQC, HMBC). The multiplicity of peaks is described using the following abbreviations: (br.) s – (broad) singlet, d – doublet, t – triplet, q – quartet, m – multiplet. NMR at various temperatures (250 to 350 K, in 10 K increments) were performed using a BCU II temperature control unit (Bruker) in combination with a liquid nitrogen evaporator for low temperatures.

3¹ and **2**[OTf]², Im₄P₄[OTf]₄³ and Cy₄P₄⁴ were prepared according to literature procedures.

1.2 Preparation of (^{CL}IM^{DIPP})P-P(DIPP) **1**



To an orange solution of **2**[OTf] (100 mg, 0.12 mmol, 1 eq.) in 3 mL THF a black solution of CoCp₂ (22.79 mg, 0.12 mmol, 1 eq.) in 3 ml THF was added dropwise. The reaction mixture was stirred for 12 h at RT and turned intensely dark red. The reaction mixture was dried under reduced pressure and 5 mL of *n*-pentane was added to the residue. CoCp₂[OTf] was removed by filtration and the solid was washed with *n*-pentane (3 x 2 ml). The collected filtrates were concentrated under reduced pressure and stored at -30 °C for two days. The product crystallized in form of dark red crystals, which were isolated by filtration. After drying under reduced pressure, **1** was obtained as air sensitive crystalline solid.

Yield: 51 mg (62 %); **melting point:** 150 °C (decomp.); **elemental analysis:** calculated: N 4.12, C 68.82, H 7.55; found: N 4.28, C 69.11, H 7.13; **UV-vis:** λ_{max} = 401 nm, 503 nm.

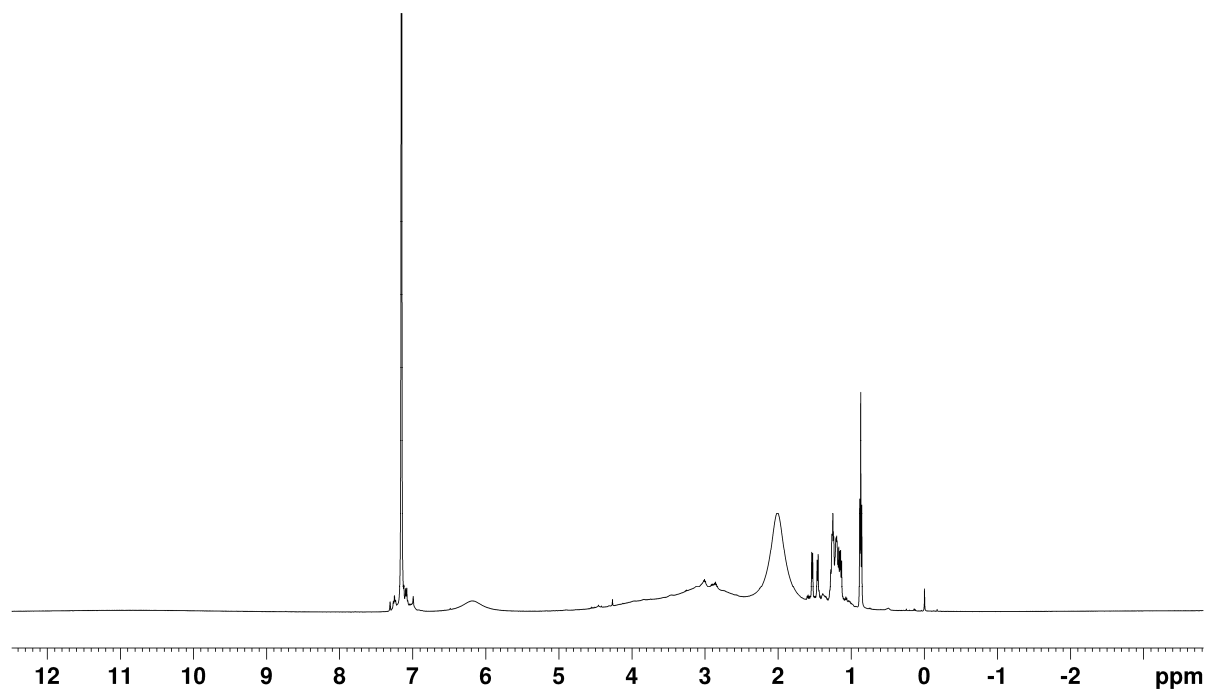


Figure S1: ¹H-NMR spectrum of **1** (C₆D₆, 300 K).

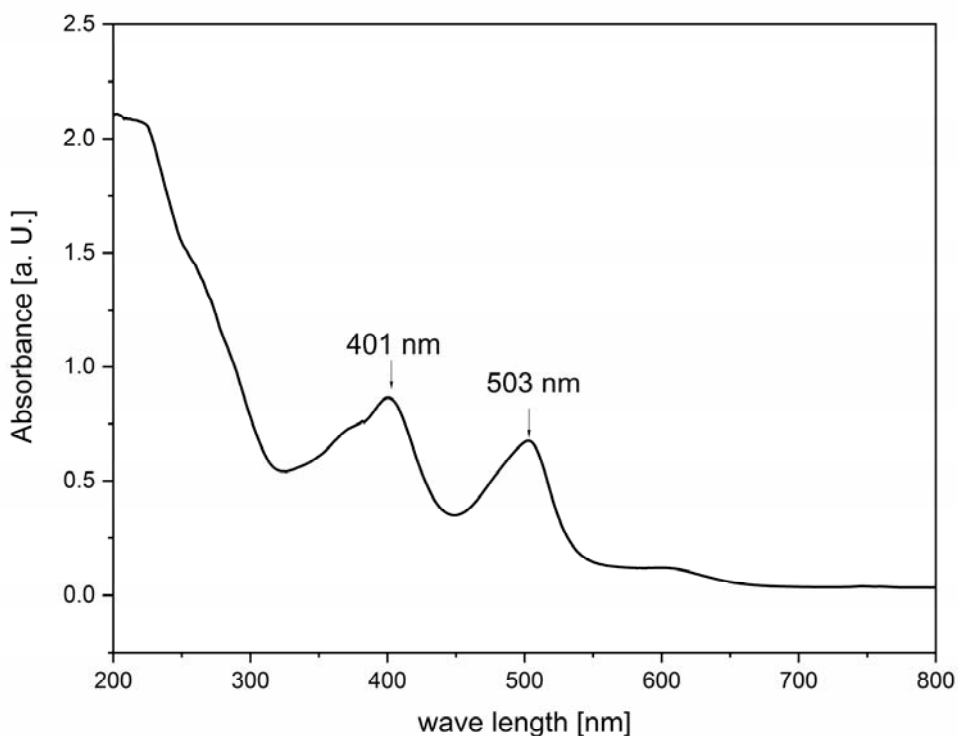


Figure S2: UV-vis spectrum of a $1.47 \cdot 10^{-4}$ M solution of **1** in *n*-pentane.

The UV-vis spectrum of **1** is shown in **Figure S2**. Compound **1** quickly reacts when exposed to atmosphere. This reaction is marked by a change in color from dark red-orange to yellow which was observed in a $1.47 \cdot 10^{-4}$ M solution of **1** in *n*-pentane. UV-vis spectra of the radical and the unidentified product after oxidation on atmosphere for 10 minutes are shown in **Figure S3**.

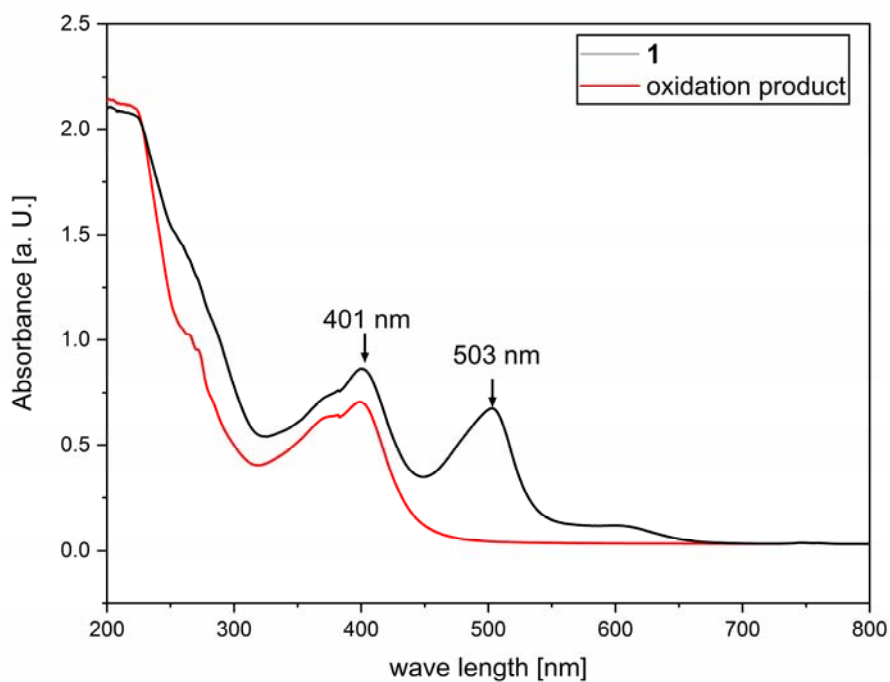


Figure S3: UV-vis spectrum of a $1.47 \cdot 10^{-4}$ M solution of **1** in *n*-pentane before (black) and after oxidation under ambient atmosphere (red).

1.3 Preparation of **1** from **3**

To a yellow suspension of **3** (100.00 mg, 0.14 mmol, 1 eq.) in 3 mL THF a solution of CoCp₂ (26.4 mg, 0.14 mmol, 1 eq.) in 3 mL THF is added. The reaction mixture quickly turns dark orange and is stirred at RT for 12 h. Additional CoCp₂ (13.2 mg, 0.07 mmol, 0.5 eq.) is added and the full conversion to **1** is monitored by NMR. The dark red suspension is filtered to remove CoCp₂Cl and the filtrate is dried under reduced pressure. The remaining black solid is dissolved in *n*-pentane, filtered and the filtrate is dried under reduced pressure. The product is obtained as a black solid in 90 % yield (85.5 mg).

It is worth noting that the radical **1** is best handled under the total exclusion of chlorinated solvents, especially CH₂Cl₂. Solutions of **1** in solvents like *n*-pentane slowly form **3** in the presence of CH₂Cl₂, which was observed in various NMR spectra.

1.4 Further investigation of the reactivity of **1**'

After removal of the previous gas phase, a solution of **1**' (15.3 mg, 0.022 mmol, 1 eq.) in 1 ml of THF in a *J Young* NMR Tube was charged with a 2 bar atmosphere of H₂ gas and vigorously shaken for several minutes. The solution was left to react at RT for 4 days. Reaction monitoring by NMR revealed no reaction. The procedure was repeated with CO gas. After another 2 days at RT, no reaction could be observed.

A suspension of Cy₄P₄ (31.87 mg, 0.07 mmol, 1 eq.) in 2 mL of THF is added to a solution of **1**' (47.5 mg, 0.07 mmol, 1 eq.) in 3 ml of THF and stirred overnight at RT. No Reaction was observed by NMR.

To a solution of **1**' (42.2 mg, 0.062 mmol, 1 eq.) in 2 mL of THF, a suspension of Im₄P₄[OTf]₄ (89.4 mg, 0.062 mmol, 1 eq.) in 3 mL of THF is added. The mixture is stirred at various temperatures and times: (i): RT, overnight; (ii): microwave, 20 min, 50 °C; (iii): microwave, 70 min, 60 °C; (iv): RT, using catalytic amounts of PPh₃, overnight and (v): microwave, 50 °C, using catalytic amounts of PPh₃, 60 min. A product could not be isolated from the resulting mixtures.

To a solution of **1**' (47.5 mg, 0.07 mmol, 1 eq.) in 2 mL of THF, a suspension of S₈ (2.23 mg, 0.009 mmol, 1/8 eq.) in 2 mL of THF is added. The mixture is stirred overnight at RT. The reaction is also performed with ¼ eq. of S₈. No product could be isolated.

Partial oxidation with trace amounts of oxygen could be observed in a sample **1**' in *n*-pentane that was stored at -30°C for several months. Crystals of the oxidation product **5** that were suitable for sc-XRD were obtained. The oxygen atom O₂ is located on both P₂ and P₃ with a occupancy of 50 % for either. For clarity, only the latter option is depicted here (**Figure S3**).

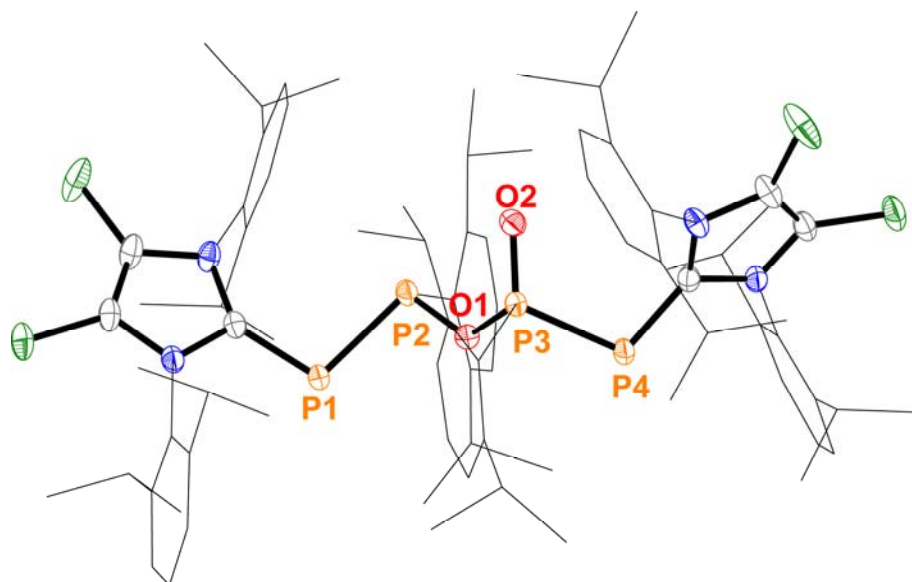
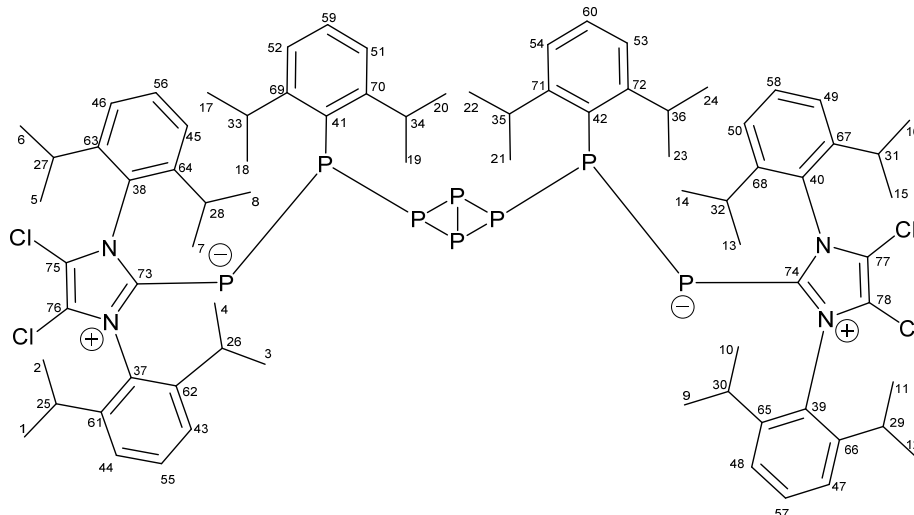


Figure S4: Molecular Structure of **5**, the partial oxidation product of **1**' (hydrogen atoms are omitted and Dipp substituents are shown as wireframes for clarity, thermal ellipsoids are displayed at 50 % probability), selected bond lengths in Å and angles in (°): P1–P2 = P3–P4 2.1796(5), P2–O1 = O1–P3 1.6533(7), P2–O2 = P3–O2 1.448(2), P1–P2–O1 = O1–P3–P4 96.75(4)°, P2–O1–P3 129.21(9)°.

1.5 Preparation of [(Cl-Im^{DIPP})P-P(DIPP)]₂-P₄ 4



To an intensely dark red solution of **1** (85.50 mg, 0.126 mmol, 1 eq.) in 3 mL *n*-pentane, a suspension of P₄ (7.78 mg, 0.063 mmol, 0.5 eq.) in 3 ml *n*-pentane was added dropwise. The reaction mixture was stirred for 12 h at RT and turned into a dark yellow suspension. The solution was filtered and the product was obtained by recrystallization from the filtrate at -30 °C as a yellow solid. The product is an inseparable mixture of stereoisomers.

Yield: 68.7 mg (73.6 %); **melting point:** 161 °C (decomposition); **Raman (100 mW, 298 K, [cm⁻¹]):** could not be obtained due to fluorescence; **IR (ATR, 298 K, [cm⁻¹]):** $\nu = 3045$ (vw), 2961 (m), 2926 (w), 2865 (w), 1611 (w), 1589 (vw), 1464 (w), 1381 (w), 1362 (w), 1320 (w), 1301 (w), 1283 (vs), 1177 (vw), 1165 (vw), 1151 (vw), 1102 (vw), 1060 (w), 1048 (vw), 983 (vw), 936 (vw), 902 (vw), 800 (s), 776 (vw), 766 (vw), 742 (w), 732 (w), 672 (m), 654 (w), 630 (vw), 600 (vw), 542 (vw), 517 (w), 472 (w), 428 (m); **¹H NMR (THF-D₈, 300 K, in ppm):** 0.84 (3H, d, ³J_{HH} = 7 Hz, CH₃); 0.88 (t, ³J_{HH} = 7 Hz, *n*-pentane); 0.93 (3H, d, ³J_{HH} = 7 Hz, CH₃); 0.96 (3H, d, ³J_{HH} = 7 Hz, CH₃); 1.00 (6 H, m, CH₃); 1.07 (3H, d, ³J_{HH} = 7 Hz, CH₃); 1.10 (3 H, d, ³J_{HH} = 7 Hz, CH₃); 1.14 (18H, m, CH₃); 1.18-1.24 (18H, m, CH₃); 1.27 (6H, br. d, ³J_{HH} = 7 Hz, CH₃); 1.32 (6H, br. d, ³J_{HH} = 7 Hz, CH₃); 1.41 (3H, d, ³J_{HH} = 7 Hz, CH₃); 2.56 - 3.03 (10H, m, CH); 3.28-3.28 (2 H, m, CH); 6.68-7.55 (18H, m, Phenyl-H); **³¹P NMR (THF-D₈, 300 K, in ppm):** Mixture of two isomers in a ratio of 15/4. **minor isomer:** ABMM'XX'YZ spin system; $\delta_A = -326.3$ (1P, dddd, ¹J_{AB} = -173 Hz, ¹J_{AM} = -177 Hz, ¹J_{AM'} = -172 Hz, ²J_{AX} = 84 Hz, ²J_{AX'} = 87 Hz, ³J_{AY} = -11 Hz, ³J_{AZ} = -9 Hz), $\delta_B = -322.2$ (1P, m, ¹J_{BM} = -176 Hz, ¹J_{BM'} = -189 Hz, ²J_{BX} = 30 Hz, ²J_{BX'} = 35 Hz, ³J_{BY} = 6 Hz, ³J_{BZ} = -4 Hz), $\delta_{M/M'} = -142.5$ (2P, m, ²J_{MM'} = -8 Hz, ¹J_{MX} = -90 Hz, ³J_{MX'} = 138 Hz, ²J_{MY} = -24 Hz, ⁴J_{MZ} = 8 Hz, ³J_{M'X} = 161, ¹J_{M'X'} = -81 Hz, ⁴J_{M'Y} = 5 Hz, ²J_{M'Z} = -100 Hz), $\delta_{X/X'} = -53.9$ (1P, m, ⁴J_{XX'} = 5 Hz, ¹J_{XY} = -275 Hz, ⁵J_{XZ} = -6 Hz, ⁵J_{X'Y} = 45 Hz, ¹J_{X'Z} = -277 Hz), $\delta_Y = -39.9$ (1P, m), $\delta_Z = -39.8$ (1P, m); **major isomer:** A₂MM'XX'YZ spin system; $\delta_A = -321.1$ (2P, m, ¹J_{AM} = -172 Hz, ¹J_{AM'} = -172 Hz, ²J_{AX} = 65 Hz, ²J_{AX'} = 77 Hz, ³J_{AY} = -8 Hz, ³J_{AZ} = -8 Hz), $\delta_{M/M'} = -139.6$ (2P, m, ²J_{MM'} = 5 Hz, ¹J_{MX} = -101 Hz, ³J_{MX'} = 91 Hz, ²J_{MY} = 35 Hz, ⁴J_{MZ} = -13 Hz, ³J_{M'X} = 63 Hz, ¹J_{M'X'} = -156 Hz, ⁴J_{M'Y} = -30 Hz, ²J_{M'Z} = 59 Hz), $\delta_{X/X'} = -47.3$ (2P, m, ⁴J_{XX'} = 12 Hz, ¹J_{XY} = -276 Hz, ⁵J_{XZ} = 8 Hz, ⁵J_{X'Y} = -7 Hz, ¹J_{X'Z} = -282 Hz, ⁶J_{YZ} = -4 Hz), $\delta_Y = -42.8$ (1P, m), $\delta_Z = -42.9$ (1P, m); **³¹P{¹H} NMR (THF-D₈, 300 K, in ppm):** Mixture of two isomers in a ratio of 15/4. **minor isomer:** ABMM'XX'YZ spin system; $\delta_A = -326.3$ (1P, dddd, ¹J_{AB} = -173 Hz, ¹J_{AM} = -177 Hz, ¹J_{AM'} = -172 Hz, ²J_{AX} = 84 Hz, ²J_{AX'} = 87 Hz, ³J_{AY} = -11 Hz, ³J_{AZ} = -9 Hz), $\delta_B = -322.2$ (1P, m, ¹J_{BM} = -176 Hz, ¹J_{BM'} = -189 Hz, ²J_{BX} = 30 Hz, ²J_{BX'} = 35 Hz, ³J_{BY} = 6 Hz, ³J_{BZ} = -4 Hz), $\delta_{M/M'} = -142.5$ (2P, m, ²J_{MM'} = -8 Hz, ¹J_{MX} = -90 Hz, ³J_{MX'} = 138 Hz, ²J_{MY} = -24 Hz, ⁴J_{MZ} = 8 Hz, ³J_{M'X} = 161, ¹J_{M'X'} = -81

Hz, $^4J_{M'Y} = 5$ Hz, $^2J_{M'Z} = -100$ Hz), $\delta_{X/X'} = -53.9$ (1P, m, $^4J_{XX'} = 5$ Hz, $^1J_{XY} = -275$ Hz, $^5J_{XZ} = -6$ Hz, $^5J_{X'Y} = 45$ Hz, $^1J_{X'Z} = -277$ Hz), $\delta_Y = -39.9$ (1P, m), $\delta_Z = -39.8$ (1P, m); **major isomer:** $A_2MM'XX'YZ$ spin system; $\delta_A = -321.1$ (2P, m, $^1J_{AM} = -172$ Hz, $^1J_{AM'} = -172$ Hz, $^2J_{AX} = 65$ Hz, $^2J_{AX'} = 77$ Hz, $^3J_{AY} = -8$ Hz, $^3J_{AZ} = -8$ Hz), $\delta_{M/M'} = -139.6$ (2P, m, $^2J_{MM'} = 5$ Hz, $^1J_{MX} = -101$ Hz, $^3J_{MX'} = 91$ Hz, $^2J_{MY} = 35$ Hz, $^4J_{MZ} = -13$ Hz, $^3J_{M'W} = 63$ Hz, $^1J_{M'X'} = -156$ Hz, $^4J_{M'Y} = -30$ Hz, $^2J_{M'Z} = 59$ Hz), $\delta_{X/X'} = -47.3$ (2P, m, $^4J_{XX'} = 12$ Hz, $^1J_{XY} = -276$ Hz, $^5J_{XZ} = 8$ Hz, $^5J_{X'Y} = -7$ Hz, $^1J_{X'Z} = -282$ Hz, $^6J_{YZ} = -4$ Hz), $\delta_Y = -42.8$ (1P, m), $\delta_Z = -42.9$ (1P, m); **$^{13}C\{^1H\}$ NMR (THF-D₈, 300 K, in ppm):** $\delta = 24.0$ (6C, br. s, C1-24), 24.2 (6C, br. s, C1-24), 24.4 (2C, s, C1-24), 24.6 (1C, s, C1-24), 25.9 (1C, s, C1-24), 26.36 (2C, s, C1-24), 26.9 (2C, s, C1-24), 27.0 (3C, br. s, C1-24), 27.3 (1C, s, C1-24), 29.7-29.9 (4C, m, C25-36), 30.0 (1C, s, C25-36), 31.5 (1C, s, C25-36), 31.8 (1C, s, C25-36), 32.1 (2C, s C25-36), 32.4 (2C, s, C25-36), 35.5-35.9 (1C, m, C25-36), 115.8 (2C, s, C75-76), 115.6 (2C, s, C77-78), 116.6 (1C, d, $^3J_{CP} = 7$ Hz, C51-54), 116.7 (1C, d, $^3J_{CP} = 7$ Hz, C51-54), 121.99 (1C, d, $^3J_{CP} = 7$ Hz, C51-54), 122.15 (1C, d, $^3J_{CP} = 7$ Hz, C51-54), 125.3 (2C, s, C43-50), 125.4 (4C, s, C43-50), 125.5 (4C, s, C43-50), 125.7 (2C, s, C43-50), 130.6 (1C, s, C60), 130.7 (1C, s, C59), 131.9 (1C, s, C58), 131.8 (2C, br. s, C56/57), 131.6 (1C, s, C55), 140.3-140.7 (2C, m, C41/42), 147.5 - 148 (8C, m, C61-68), 152.8 (4C, dd, $^2J_{CP} = 32$ Hz, $^3J_{CP} = 2$ Hz, C69-72), 154.8-155.1 (4C, m, C37-40), 173.2 (2C, br. dd, $^1J_{CP} = -120$ Hz, $^2J_{CP} = 20$ Hz, C73/74); **elemental analysis:** calculated: N 3.77, C 63.08, H 6.92, S 0; found: N 3.57, C 62.95, H 6.42, S 0.32.

NMR studies at variable temperatures in the 350 K to 250 K range did not result in changes in the shape of the products resonances in the ^{31}P and $^{31}P\{^1H\}$ NMR spectra. Only slight deviations of the chemical shifts were observed (ca. 1 ppm or less, in comparison to the spectrum at 300 K).

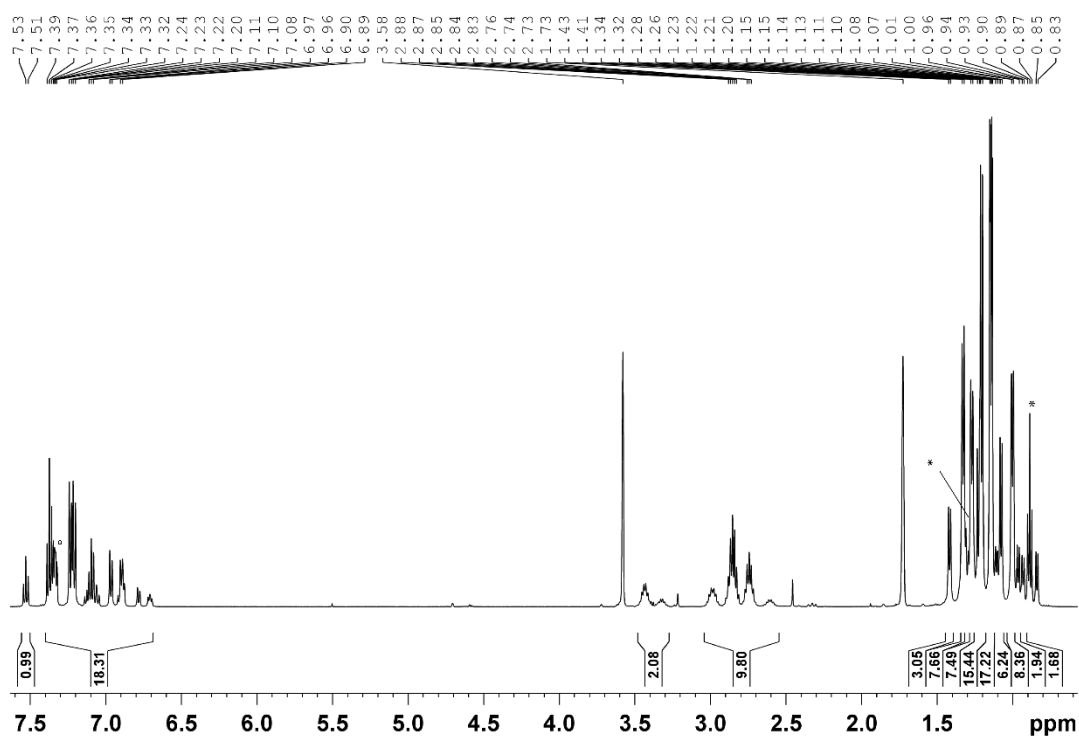


Figure S5: ^1H NMR spectrum of **4**, *: *n*-pentane, °: benzene (THF- D_8 , 300K).

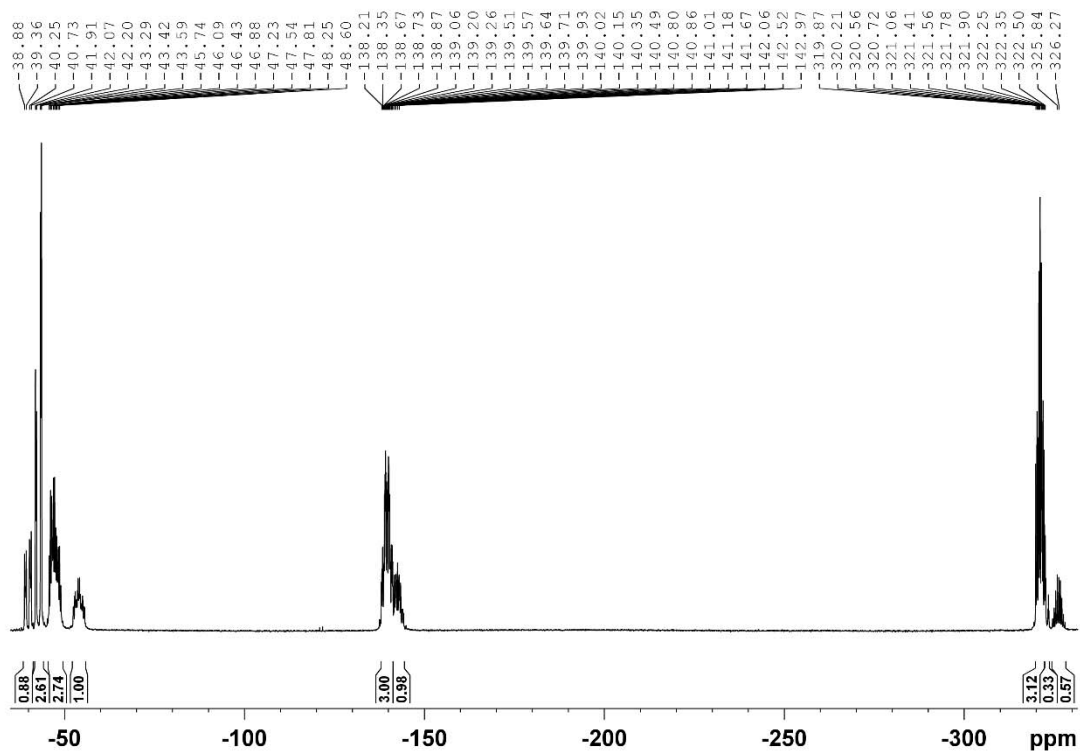


Figure S6: ^{31}P NMR spectrum of **4** (THF- D_8 , 300K).

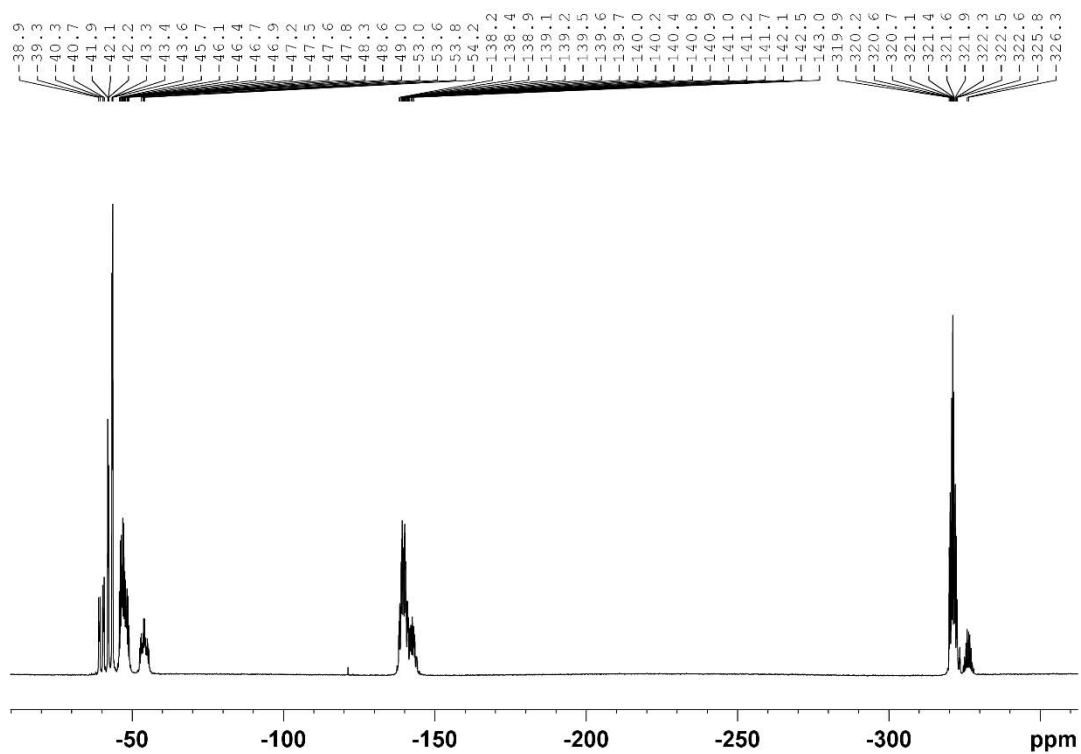


Figure S7: $^{31}\text{P}\{^1\text{H}\}$ NMR spectrum of **4** (THF- D_8 , 300K).

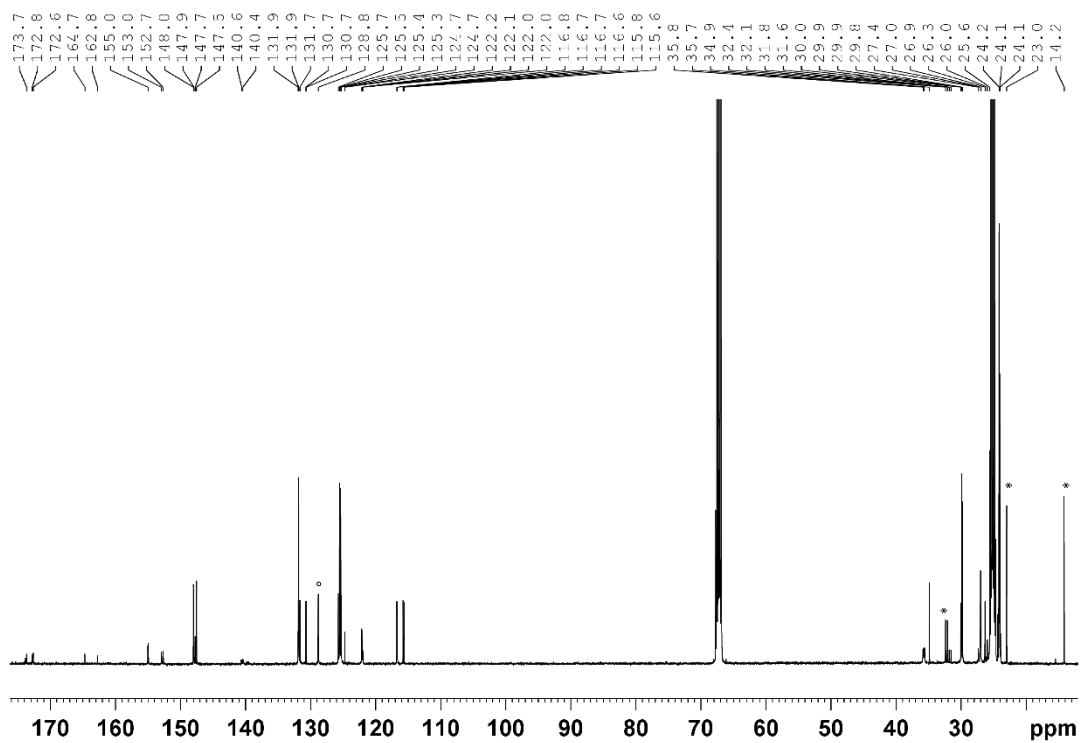


Figure S8: $^{13}\text{C}\{^1\text{H}\}$ NMR spectrum of **4**, *: *n*-pentane, °: benzene (THF- D_8 , 300K).

1.6 Preparation of **4** from **3** in a stoichiometric ratio with P₄

To a yellow solution of **3** (44.00 mg, 0.06 mmol, 1 eq.) in 3 mL THF a solution of CoCp₂ (11.61 mg, 0.06 mmol, 1 eq.) in 3 mL THF was added. The reaction mixture quickly turns dark orange and is stirred at RT for 30 minutes. Then, a suspension of P₄ (3.8 mg, 0.03 mmol, 0.5 eq.) in 3 ml THF is added dropwise. The reaction mixture is stirred for 12 h at RT. The reaction mixture is filtered and the yellow filtrate dried under reduced pressure, dissolved in ca. 10 mL of *n*-pentane, and filtered again. The product precipitates from the *n*-pentane filtrate at -30 °C and is obtained as a yellow solid in 28.5 % yield (13 mg).

1.7 Preparation of **4** from **3** in a 1 to 1 ratio with P₄

To a yellow solution of **3** (20.00 mg, 0.03 mmol, 1 eq.) in 2 mL THF a solution of CoCp₂ (5.31 mg, 0.03 mmol, 1 eq.) in 2 mL THF is added. The reaction mixture quickly turns dark orange and is stirred for 3 h at RT. Then, a suspension of P₄ (3.46 mg, 0.03 mmol, 1 eq.) in 3 ml THF is added dropwise. The reaction mixture is stirred for 12 h at RT. The reaction mixture is filtered and the yellow filtrate contains product **4** and P₄ (**Figure S8**). Apparently, no further addition of radical to the P₈ moiety is possible under these conditions.

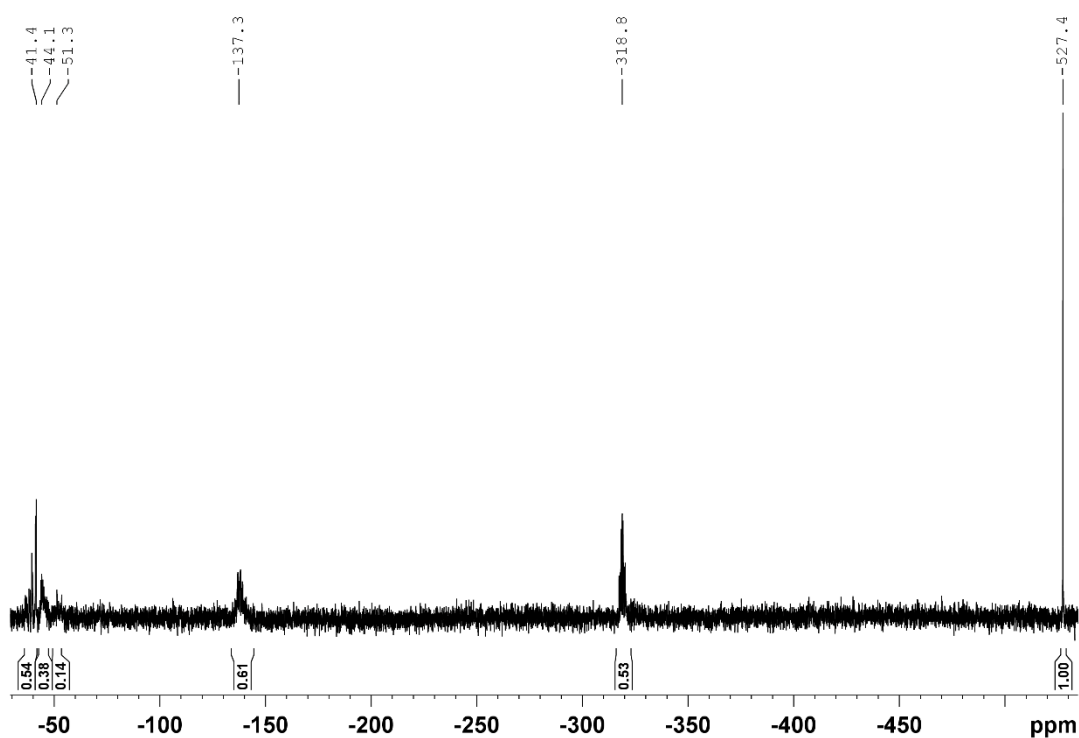


Figure S9: ³¹P NMR spectrum of the filtrate (C₆D₆-capillary, *n*-pentane, 300 K).

1.8 Investigation of the ratio of isomers of **4**

Room temperature NMR spectra of **4** were also recorded in the solvents THF-D₈, *n*-hexane, *n*-pentane, and CH₃CN. A C₆D₆-Capillary was used for non-deuterated solvents. In all spectra, the shifts are changed slightly, but the splitting pattern remains unchanged.

The appearance of two sets of signals in the ³¹P{¹H} NMR (Toluene-D₈, 300 K - 250 K and 300 K - 350 K, in 10 K increments) was investigated using high and low temperature NMR in the temperature range from 250 K to 350 K. Only slight changes of the chemical shifts were observed and the splitting pattern remained virtually unchanged, compared to the room temperature spectra.

It appears that the energetic barrier of conversion of one isomer to the other is too high as to be affected in this temperature range. In an attempt to influence the ratio of isomers (as indicated by the integral intensity of the respective resonances in the ³¹P NMR spectra) during the formation of the product, the reaction of **1** and P₄ was conducted at high and low temperatures.

1.8.1 Reaction of **1** and P₄ at low temperatures

P₄ (6.37 mg, 0.05 mmol, 0.5 eq.) is suspended in ca. 3 mL of *n*-pentane and cooled in an ethanol/liquid N₂ cooling bath at -114 °C. A strongly colored solution of **1** (70.0 mg, 0.10 mmol, 1 eq.) in ca. 2 mL of *n*-pentane is slowly added and the reaction mixture is stirred and allowed to slowly heat up to RT overnight. The reaction mixture is filtered, the filter residue is washed with a small amount of *n*-pentane and dried under reduced pressure to obtain the product as a yellow solid in 75.3 % yield (57.5 mg).

Compared to the reaction conducted at RT, the reaction at low temperatures yielded a similar ratio of both isomers, as indicated by the integral intensity of the signal groups in the ³¹P NMR.

1.8.2 Reaction of **1** and P₄ at elevated temperatures

P₄ (3.86 mg, 0.03 mmol, 0.5 eq.) is suspended in ca. 7 mL of *n*-hexane and refluxed at ca. 69 °C. A strongly colored solution of **1** (42.4 mg, 0.06 mmol, 1 eq.) in ca. 5 mL of *n*-hexane is added and the reaction mixture is stirred and refluxed for 1 h. Afterwards, the reaction mixture is allowed to cool and stirred at RT overnight. The yellow reaction mixture is reduced under reduced pressure and filtered to remove a very small amount of brown solid. NMR analysis of the brown-yellow filtrate shows white phosphorus, traces of **4** and the decomposition of **1**.

2 Iteration of NMR spectra

The ^{31}P $\{^1\text{H}\}$ NMR spectrum of **4** (THF- D_8 , 300 K) was iteratively fitted using the software *gNMR* v5.0.6 (Ivorysoft). Both isomers were iterated simultaneously, as the signals partially overlap. The fitted parameters are given in **Tables S1-4**. The relative concentration of both isomers (15/4) was also confirmed by iteration.

Table S1: Minor product (ABMM'XX'YZ spin system), chemical shifts and widths.

Title	multiplicity	Shift [ppm]	Width
A	1	-326.29	12.47
B	1	-322.15	4.89
M	1	-142.55	13.35
M'	1	-142.55	4.91
X	1	-53.95	11.46
X'	1	-53.95	35.12
Y	1	-39.85	9.2
Z	1	-39.84	6.89

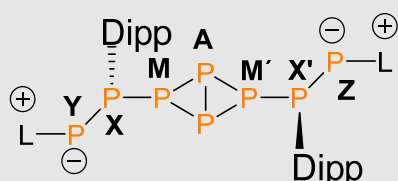
Table S2: Minor product (ABMM'XX'YZ spin system), shifts and widths.

	A	B	M	M'	X	X'	Y	Z					
A	-	<p style="text-align: center; color: red;">minor product</p>											
B	$^1J_{AB}$ -172.9												
M	$^1J_{AM}$ -176.61								$^1J_{BM}$ -175.92				
M'	$^1J_{AM'}$ -171.61								$^1J_{BM'}$ -188.66	$^2J_{MM'}$ -7.85			
X	$^2J_{AX}$ 83.96								$^2J_{BX}$ 30.40	$^1J_{MX}$ -89.88	$^3J_{M'X}$ 160.52		
X'	$^2J_{AX'}$ 87.23								$^2J_{BX'}$ 35.00	$^3J_{MX'}$ 137.73	$^1J_{M'X'}$ -80.53	$^4J_{XX'}$ 4.60	
Y	$^3J_{AY}$ -11.01								$^3J_{BY}$ 5.76	$^2J_{MY}$ -24.16	$^4J_{M'Y}$ 4.37	$^1J_{XY}$ -275.23	$^5J_{X'Y}$ 44.69
Z	$^3J_{AZ}$ -9.25								$^3J_{BZ}$ -3.86	$^4J_{MZ}$ 7.81	$^2J_{M'Z}$ -100.37	$^5J_{XZ}$ -5.63	$^1J_{X'Z}$ -276.94

Table S3: Major product ($A_2MM'XX'YZ$ spin system), chemical shifts and widths.

Title	multiplicity	Shift [ppm]	Width
A	2	-321.12	13.82
M	1	-139.64	10.99
M'	1	-139.63	21.39
X	1	-47.26	200.43
X'	1	-47.26	16.7
Y	1	-42.87	5.8
Z	1	-42.86	10.56

Table S4: Major product ($A_2MM'XX'YZ$ spin system), coupling constants.

	A	M	M'	X	X'	Y	Z						
A	-	 <p style="text-align: center;">major product</p>											
M	$^1J_{AM}$ -171.36							-					
M'	$^1J_{AM'}$ -171.66							$^2J_{MM'}$ 4.47	-				
X	$^2J_{AX}$ 65.45							$^1J_{MX}$ 102.98	$^3J_{M'X}$ 62.77	-			
X'	$^2J_{AX'}$ 77.48							$^3J_{MX'}$ 90.75	$^1J_{M'X'}$ -155.87	$^4J_{XX'}$ 12.02	-		
Y	$^3J_{AY}$ -8.30							$^2J_{MY}$ 35.03	$^4J_{M'Y}$ -30.00	$^1J_{XY}$ -276.56	$^5J_{X'Y}$ -6.64	-	
Z	$^3J_{AZ}$ -8.12							$^4J_{MZ}$ -13.23	$^2J_{M'Z}$ 58.72	$^5J_{XZ}$ 7.65	$^1J_{X'Z}$ -282.29	$^6J_{YZ}$ -3.88	-

3 Electrochemical procedures and Data

All electrochemical (EC) measurements such as cyclic voltammetry (CV) and square wave voltammetry (SWV) were performed in a Glovebox Pure Lab HE GP-1 SR (Innovative Technology, USA) in an atmosphere of purified nitrogen (< 0.1 ppm O_2 ; < 0.1 ppm H_2O). The glovebox was equipped with military grade BNC feedthroughs in a custom-made gas tight flange for low noise electrical connection of the electrochemical cells inside. EC cells were connected to a PGSTAT302 (Metrohm Autolab, Utrecht, The Netherlands) $E = \pm 10$ V, $U = \pm 35$ V. NOVA Software (Metrohm Autolab) Version 1.11.2 was used to control the potentiostat and magnetic stirring. Data analysis of the electrochemical data was performed using OriginPro 2019 (OriginLab Cooperation, Northampton, MA, USA).

EC measurements were performed in 10 mL electrochemical cells using platinum disk electrodes (1.6 mm diameter, ALS Co. Ltd., Japan) as working electrodes. The electrodes were polished with 1 μ m Diamond polishing paste and then 0.05 μ m polishing alumina on separate polishing pads prior to use. A Pt wire coil (200 mm length, 0.5 mm width) was used as counter electrode without separation. A reference electrode, consisting of a silver wire in a solution of 0.01 M $AgNO_3$ in 0.1 M $[Bu_4N][OTf]$ supporting electrolyte solution (in CH_2Cl_2) and separated from the substrate solution by a Vycor Frit, was used. Ferrocene was used to reference the potentials obtained in CV and SWV experiments to a potential of $E_{1/2} = 0$ V according to IUPAC convention.

$[nBu_4N][OTf]$ was pre-dried at least 5 times by dissolving in CH_2Cl_2 and evaporating the solvent to high vacuum at 80 $^{\circ}C$. Final drying and removal of HOTf traces was achieved by dissolving in dry benzene and refluxing this solution in a Soxhlet apparatus for 5 days with vacuum activated molecular sieves in the extraction thimble renewed every day. Prior to each measurement, the electrolyte stock solution is passed through a Pasteur pipette with an activated ($1 \cdot 10^{-3}$ mbar, 350 $^{\circ}C$, 24 h) aluminum oxide bed ($D = 5$ mm; $L = 70$ mm) in the glove box before the substrate is added.

In the second cycle CV of **2**[OTf] (**Figure 2** in the paper, black), a reversible one-electron reduction is observed at $E_{1/2} = -0.862$ V (vs. $E_{1/2}(\text{FeCp}_2/\text{FeCp}_2^+)$). SWV measurements of the reversible process shows its formal potential of $E_p = -0.859$ V. The reversibility was proven using the Randles–Ševčík equation (**Figure S9**). Cobaltocene, which has a formal potential of -1.33 V (vs. $E_{1/2}(\text{FeCp}_2/\text{FeCp}_2^+)$)⁵ in CH_2Cl_2 , was chosen as a suitable reduction agent. Based on experimental results following the chemical reduction of **2**[OTf] with cobaltocene, the reduction process observed above was assigned to the formation of **1**.

The isolated radical **1**[•] was also analyzed using the same methods (**Figure 2** in the paper, red). The CV reveals a reduction process at a potential of $E_{1/2} = -0.913$ V (vs. $E_{1/2}(\text{FeCp}_2/\text{FeCp}_2^+)$). The SWV shows the same process at a potential of $E_p = -0.917$ V (vs. $E_{1/2}(\text{FeCp}_2/\text{FeCp}_2^+)$). This process is assigned to the oxidation and re-reduction of radical **1**.

Although this process fulfills the Randles–Ševčík equation (**Figure S10**), the CV curve is noticeably broadened and slightly deformed, with the peak-to-peak separation of 125.4 mV strongly exceeding the expected range for reversible processes (57 mV)⁶ and the separation observed in the CV of **2**[OTf] (62 mV). Therefore, it is designated as pseudo-reversible.

The broadening of a CV Curve may be indicative of a deviation from a fully diffusion-controlled process. This could be caused by a different coefficient of diffusion of the radical. Its heightened reactivity could also cause side reactions with the products that form during the CV process. These would not directly be visible in the CV as a chemical follow-up reaction requires no electron-exchange with the electrode, but could, for example, change the concentration of **2**⁺ that is available for re-reduction. Both of these effects could contribute to a broadened CV curve.

We suspect that when starting the measurement with the radical species **1**, the effects of these properties (coefficient of diffusion and reactivity) are more pronounced due to the high initial concentration of the radical. In contrast, the shape of the CV curve is not broadened for the measurement of **2**⁺, possibly because only small amounts of the radical are produced and re-oxidized near the electrode.

Please note that both CVs still fulfill the Randles–Ševčík equation which is a criterium for reversibility and indicates a diffusion controlled process.

A reversible oxidation of **2**[OTf] to a “**2**⁺” species was not observed in the potential range of -2 V to 2 V.

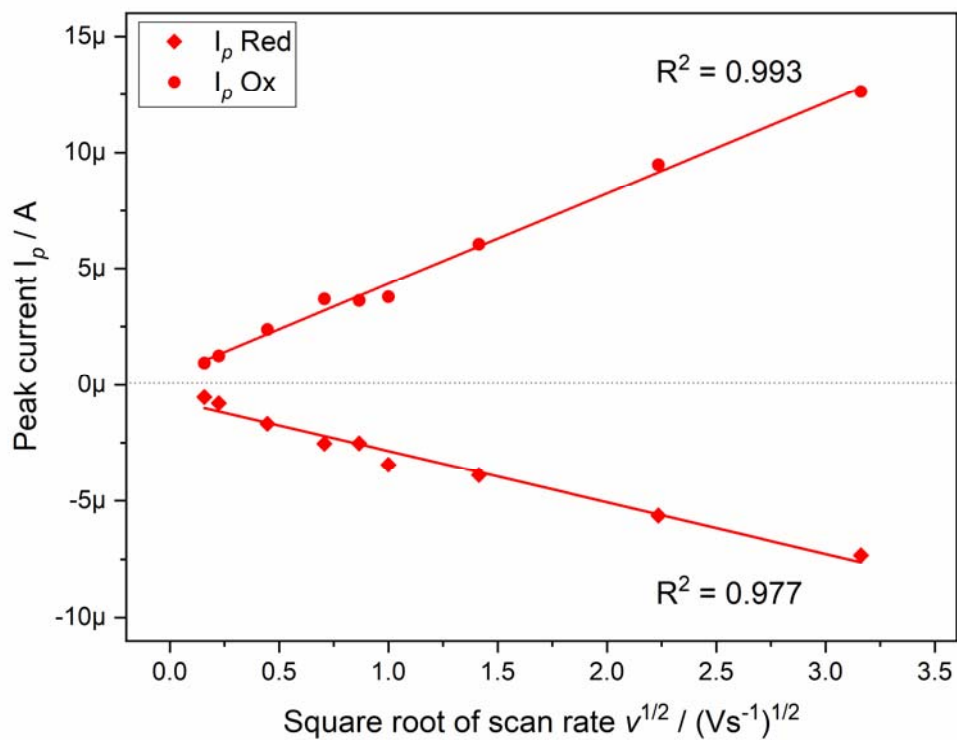


Figure S10: Randles–Ševčík plot for the reversible reduction and oxidation of **1** in CH_3CN at a 1.6 mm Pt disc electrode, scan rate $v = 0.2 \text{ V/s}$.

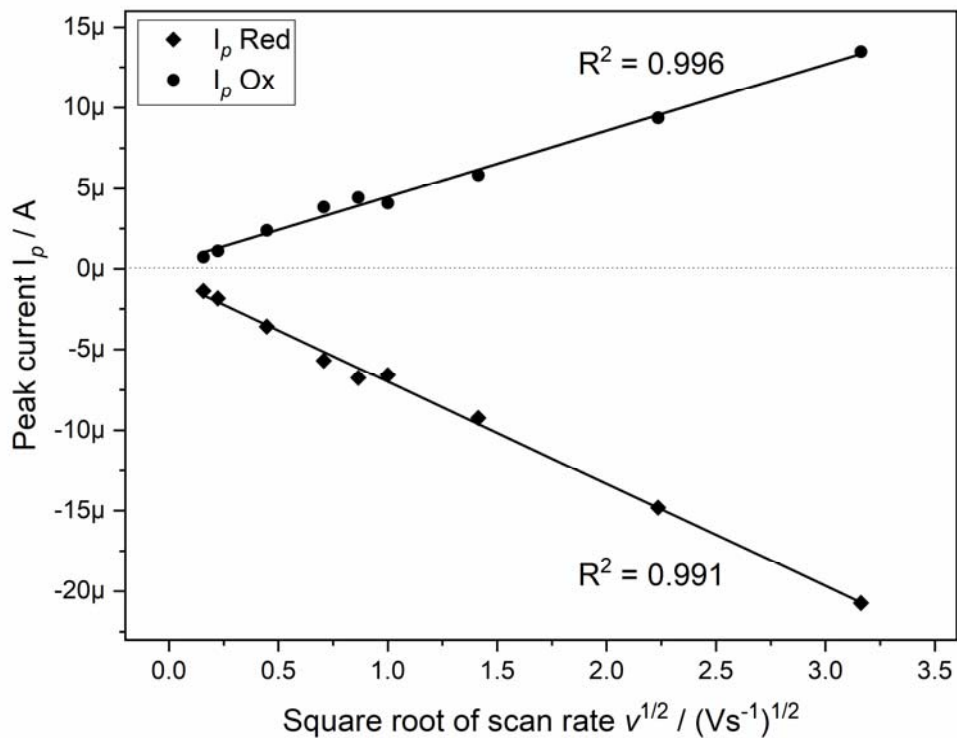


Figure S11: Randles–Ševčík plot for the reversible reduction and oxidation of **2[OTf]** in CH_3CN at a 1.6 mm Pt disc electrode, scan rate $v = 0.2 \text{ V/s}$.

4 DFT calculation of molecular orbitals and spin density and computational details

4.1 Computational methods

The geometries and energies of the radical included in this study were fully optimized at the RI-UBP86-D3/def2-TZVP level of theory. For comparison, some calculations have been also done using the X-ray coordinates. The calculations have been performed by using the program TURBOMOLE version 7.0⁷. For the calculations we have used the BP86⁸ functional with the D3 correction for dispersion⁹. In order to reproduce solvent effects, we have used the conductor-like screening model COSMO¹⁰, which is a variant of the dielectric continuum solvation models. The minimum nature of the complexes and compounds have been confirmed by doing frequency calculations. The Wiberg bond index¹¹ calculations were performed using the NBO7.0 program¹².

4.2 Discussion of the frontier orbitals and spin density

In **Figure S12** the plots of HOMO, SOMO and LUMO for **1**[·] are represented. It can be observed that the HOMO has π -character and it is mostly localized at the P atoms (P=P double bond) with some participation of the five membered ring (5R). The SOMO corresponds to the combination of antibonding $\pi^*(\text{P}=\text{P})$ and bonding $\pi(\text{P}=\text{C})$ with some participation of the five-membered ring. Finally, the LUMO is localized at the π -systems of the bis-(isopropyl)phenyl rings. The DFT and X-ray distances are very similar, giving reliability to the level of theory (RI-PB86-D3/def2-TZVP).

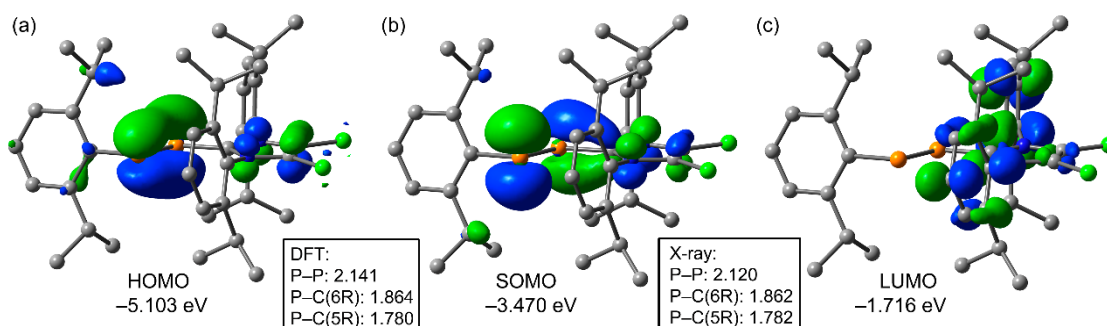


Figure S12: MOs computed for **1**[·] and their energies at the RI-BP86-D3/def2-TZVP level of theory. Distances in Å.

The spin density plot is given in **Figure S13** along with the Wiberg bond indices for the C-P-P-C system. It can be observed that the spin is basically localized at the P atom (65%) bonded to the six membered ring (6R). Some spin is delocalized to the other P atom (8%) and the five membered ring (21%). The WBIs confirm that the bond order is higher than 1 in the P-P and P-C(5R) bonds, disclosing some double bond character, in line with the HOMO and SOMO orbitals. In contrast, the P-C(6R) WBI is 0.94, confirming its single bond character.

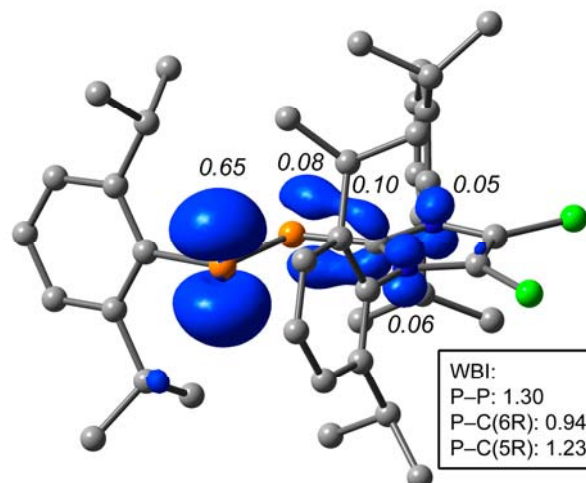


Figure S13: Spin density plot of $\mathbf{1}^\bullet$ with indication of the spin density values (in italics) for some atoms at the RI-BP86-D3/def2-TZVP level of theory. The P-P and P-C WBIs are also indicated.

4.3 Mechanistic Studies

The mechanistic study for the formation of **4** reveals a two-step mechanism involving the formation of a non-covalent complex in the first step. Initially, one molecule of $\mathbf{1}^\bullet$ interacts with P_4 , resulting in a supramolecular assembly $[\mathbf{1}^\bullet \cdots \text{P}_4]^\bullet$ that is well pre-organized for subsequent P-P bond formation, with a $\text{P} \cdots \text{P}$ distance of 2.948 Å, as illustrated in Figure S14. This process is exergonic ($\Delta G = -4.2$ kcal/mol). The second step, which is barrierless (see energy profile in Figure S15) and significantly more exergonic ($\Delta G = -37.6$ kcal/mol), involves the coupling of the supramolecular radical $[\mathbf{1}^\bullet \cdots \text{P}_4]^\bullet$ with a second molecule of $\mathbf{1}^\bullet$, leading to the formation of compound **4**.

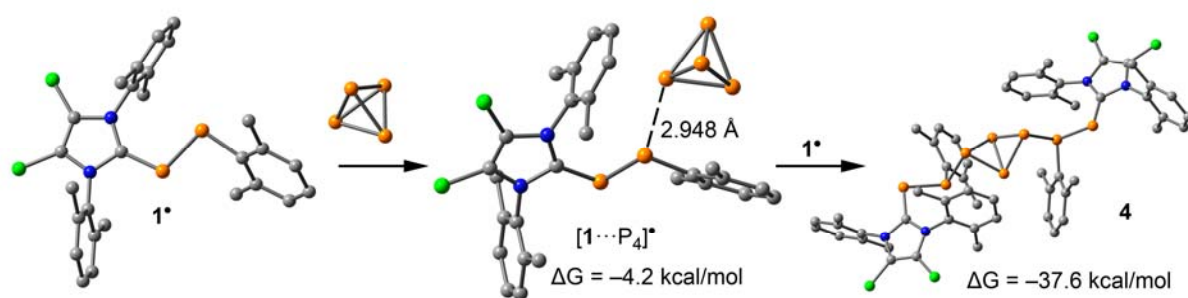


Figure S14: Optimized geometries and Gibbs energies involved in the transformation of $\mathbf{1}^\bullet$ and P_4 into **4**.

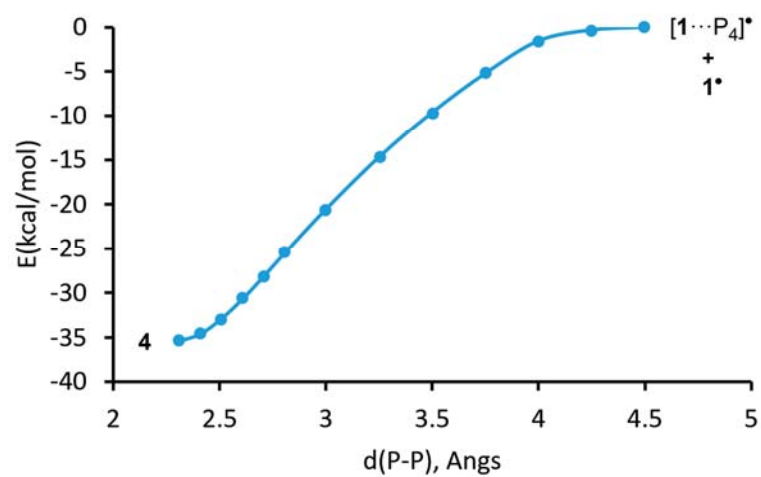


Figure S15: Energy profile for the transformation of $[1 \cdots P_4]^+ + 1^+$ and P_4 into **4**. The y-axis shows relative energies references to the starting material.

4.3 Cartesian Coordinates of the optimized radical:

Cl	13.62891824	10.49030607	14.08203367
Cl	13.57158983	10.61067431	10.53467229
P	14.51398571	4.42106848	13.77380486
P	14.47477209	5.39377193	11.86735386
N	13.99701923	7.99671597	11.11552475
N	14.00108701	7.90315214	13.31438111
C	14.91967522	2.76939621	13.00915643
C	13.89210984	1.93687287	12.49713723
C	12.43256596	2.37193647	12.48306852
H	12.39943999	3.39571824	12.89056940
C	11.56835919	1.49027796	13.39773129
H	11.54646501	0.44743206	13.04714395
H	10.53191845	1.85960717	13.42195173
H	11.95924496	1.49135431	14.42522311
C	11.86989497	2.43484030	11.05485617
H	12.47596749	3.10370712	10.42795258
H	10.83641074	2.81265275	11.06407973
H	11.86038883	1.44136188	10.58118062
C	14.22898355	0.67323782	11.99331286
H	13.44296218	0.02521741	11.59951503
C	15.54970889	0.23123670	11.98199587
H	15.79500265	-0.75294884	11.57878504
C	16.55792120	1.05083224	12.48796023
H	17.59114560	0.69943950	12.47241301
C	16.26535973	2.31671947	13.01011583
C	17.39055302	3.20510065	13.52416231
H	16.91569317	3.97325223	14.16215693
C	18.41685843	2.45866281	14.38752346
H	17.92573432	1.90249117	15.19817380
H	19.12403080	3.17172386	14.83670869
H	19.00858390	1.74371577	13.79630230
C	18.07139882	3.94535242	12.36053700
H	18.52783484	3.23004025	11.65905805
H	18.86114295	4.61598933	12.73259517
H	17.34200048	4.54961410	11.80223648
C	14.14388444	7.11437112	12.18231592
C	13.81719369	7.56975354	9.75581810
C	14.94961130	7.42905748	8.93683852
C	16.34909304	7.71003526	9.45654032
H	16.28177640	7.82510168	10.54864204
C	17.30480196	6.53737583	9.18617361
H	16.88985503	5.60031511	9.58024979
H	18.27328788	6.71695213	9.67484975
H	17.49496393	6.40789198	8.11045310
C	16.88677416	9.03077647	8.87745001
H	16.97500283	8.96926174	7.78255900
H	17.88309215	9.25498147	9.28594098
C	16.21689927	9.86883925	9.11597666
C	14.73440868	7.01951980	7.61526067
H	15.58698995	6.90088567	6.94550643
C	13.44804863	6.75207415	7.14914283
H	13.30264819	6.42922682	6.11710484
C	12.34668578	6.88541888	7.99453100
H	11.34763618	6.66057993	7.61869080
C	12.50548129	7.29780459	9.32261032
C	11.30802091	7.40820737	10.25451580
H	11.64604770	7.85756035	11.19959250
C	10.75198369	6.01412060	10.59267805
H	10.37716797	5.50730109	9.69125318
H	9.91975562	6.09772426	11.30729171
H	11.53184331	5.38105580	11.03845061
C	10.21874447	8.33079139	9.68485966
H	10.62392597	9.32611188	9.45514805
H	9.40402794	8.44925672	10.41385265
H	9.78304903	7.91858666	8.76319588
C	13.78925313	9.29026595	11.58112400
C	13.79494602	9.23906487	12.94434545
C	13.95336052	7.43664483	14.67202132
C	12.76320331	6.83249428	15.12672481
C	11.57182530	6.64128190	14.19874477
H	11.97512186	6.45719701	13.19145905
C	10.70439319	7.91104959	14.13056557
H	10.26722505	8.13521754	15.11485431
H	9.88189140	7.77221623	13.41318220
H	11.28405924	8.78887315	13.81488595
C	10.72017378	5.41563595	14.55175521
H	11.34595975	4.51898955	14.66035191

H	9.99210368	5.22917082	13.75013740
H	10.15265129	5.56070248	15.48332466
C	12.74099216	6.40293941	16.45791093
H	11.84778541	5.91952805	16.85164897
C	13.85679361	6.55667334	17.28019416
H	13.81983587	6.20199334	18.31126693
C	15.02235942	7.14600110	16.79348127
H	15.88988837	7.24265903	17.44591872
C	15.09610027	7.60562382	15.47330257
C	16.38182159	8.19135372	14.90905304
H	16.12116317	8.79509257	14.02651292
C	17.09413174	9.12640833	15.89609932
H	16.41455279	9.90587372	16.26824163
H	17.94441586	9.61673815	15.40149269
H	17.49404210	8.57905860	16.76208677
C	17.31334447	7.06228632	14.42781079
H	17.58655445	6.40342255	15.26506445
H	18.23713184	7.48086341	14.00160667
H	16.82409629	6.44316111	13.66395560

1' (with methyl groups instead of isopropyl)

Cl	-6.93928203503680	1.05668962912075	3.90736293296254
Cl	-9.59910365492644	0.31943470843590	1.63252744147006
P	-4.94122102058425	0.06206319690868	-1.26234780524042
P	-3.02038508488643	0.86621058356886	-0.69151261456430
N	-5.69552937156856	0.66314979259021	1.50714945596487
N	-7.34378945809954	0.19403026700924	0.11415406326730
C	-5.95888891396918	0.34144697828824	0.17835469562436
C	-4.39212200432858	0.76211654306941	2.09995963469212
C	-3.69151433096238	-0.43367278493455	2.37097318997542
C	-2.39877328346348	-0.31462234851672	2.91416371823271
H	-1.82030014433011	-1.22750209815730	3.12346619199019
C	-1.84531039273539	0.94648262756069	3.17740123812723
H	-0.83010245991762	1.02027782283644	3.59601952898365
C	-2.57036507462250	2.11531669039594	2.90226962773758
H	-2.12225051081307	3.10214004710176	3.09412974548292
C	-3.86188634054801	2.04590229903975	2.35018358964376
C	-6.89367899691543	0.70742105761559	2.23694173703699
C	-7.91542106013926	0.41332107034316	1.36842958844899
C	-8.06453947510151	-0.12529805112336	-1.08509781250109
C	-8.45836365345498	0.93332881393927	-1.93217434987392
C	-9.16592974328507	0.59561522949056	-3.10076031839358
H	-9.48516460340442	1.39701471584038	-3.78470971989042
C	-9.45847051113690	-0.74377237488441	-3.39956661413451
H	-10.01123302818778	-0.98927512992341	-4.31917980788534
C	-9.04603056666131	-1.77343609426709	-2.54058187273008
H	-9.26958430389684	-2.82273439015156	-2.78736595052594
C	-8.33475198051405	-1.48281867424271	-1.36135962967420
C	-2.22040992873720	0.31443056735388	-2.28424308671329
C	-2.18086390522274	1.18777770840465	-3.40766317642541
C	-1.49439673948993	0.78003169901079	-4.56874514040761
H	-1.46388083098339	1.45637419722759	-5.43829903897455
C	-0.85655749217322	-0.46681560288608	-4.62940381093311
H	-0.32134091436039	-0.76965238333060	-5.54285331680238
C	-0.90322494991648	-1.32718441520149	-3.52377354876694
H	-0.40671217360672	-2.31004446029907	-3.56965568849112
C	-1.58091057074418	-0.95629621522566	-2.34532452886835
C	-7.84708005247346	-2.55915597206248	-0.42652325487845
H	-8.29807279849254	-2.45659166592990	0.58278553446909
H	-8.09503338548301	-3.56593536538181	-0.81182582053426
H	-6.74538793519606	-2.49505979213178	-0.30292593454239
C	-8.09529087921793	2.35429610302475	-1.59024764514729
H	-8.47830213096612	2.64336140263000	-0.58952075179346
H	-6.99018212003545	2.47015476752595	-1.56502749606869
H	-8.50340285177259	3.06312455973109	-2.33489998621937
C	-4.29400066403374	-1.76868436098773	2.02841023167193
H	-5.33424169439519	-1.86051978867571	2.40254721781677
H	-4.33693068248770	-1.88927763426464	0.92298788198557
H	-3.69548272468401	-2.59955677619273	2.44658109636922
C	-4.63876929996771	3.27797863246266	1.96734563139065
H	-4.88408833166470	3.25563092220579	0.88474341307046
H	-5.59633914680256	3.34777739705353	2.52383832338255
H	-4.05540837956093	4.19564316977369	2.16987111772833
C	-2.87944734737619	2.52641104266228	-3.37193277764182
H	-2.55040542926444	3.13053389436234	-2.50000470111522
H	-2.69001654546312	3.10617555901115	-4.29697517369991
H	-3.97647633816325	2.39688906791176	-3.25660363250242
C	-1.64334871952954	-1.91090197924537	-1.17635291134075

H	-2.68039183849804	-2.28078459777120	-1.02634560719705
H	-0.98144800854740	-2.78568533037665	-1.33250875070961
H	-1.35871298719981	-1.40755417734274	-0.22811035233793

[1...P₄]

Cl	7.72839462605705	1.14280336898770	-3.37648156261058
Cl	9.96400166828522	1.27580575579599	-0.59569292813268
P	-0.48159826367553	1.68882619734584	-1.25886665633704
P	0.56480000364624	-0.24019609189087	-1.70260354101802
P	-0.26028586932558	0.12419695078682	0.33578622411899
P	1.56115900713303	1.19259444334513	-0.35940727003821
P	3.53304364442853	-0.89982311610024	0.29133483609701
P	5.03633210274038	0.10210972852426	1.47061624293402
N	6.15496049263220	0.56302128990514	-1.21504518207269
N	7.54688617352053	0.66844130801839	0.49604343610014
C	2.30826294404854	-1.55766467654497	1.49787118039808
C	1.86631220427893	-0.94518950985176	2.71449478524480
C	0.81902204611722	-1.54146012932796	3.44331823538881
H	0.48342559082574	-1.05610915251477	4.37357304015572
C	0.18779423872261	-2.71104104529994	3.00205586062008
H	-0.63347253475802	-3.15388474107701	3.58580370026478
C	0.60020117533091	-3.29914869279255	1.79976791507738
H	0.10138449863718	-4.21019861042621	1.43299018335394
C	1.64352089735428	-2.74472929943135	1.03647261496180
C	6.21688706163606	0.42765618083217	0.16759677460424
C	4.97897718110704	0.67455497561565	-2.04086455776486
C	4.2954282795973	1.91032474847215	-2.05057789587631
C	3.22112188823560	2.05111154166268	-2.95215612914280
H	2.66170015966625	2.99827721042453	-2.97430597853359
C	2.85850851638363	0.99898177002009	-3.80384514804206
H	2.01598308546805	1.12640614139059	-4.49964979351848
C	3.55045866885111	-0.22143145308070	-3.75945575788166
H	3.24491134373850	-1.05222728384407	-4.41327208419301
C	4.63218162009480	-0.40722739401241	-2.88092114162177
C	7.43066097875632	0.88171157543093	-1.71737207755648
C	8.29060276092578	0.94899429335424	-0.65030066346661
C	8.08344528343554	0.56818457866886	1.82484618519732
C	8.48806986241776	-0.70253748828812	2.28923778514407
C	9.02152943205050	-0.77283648797635	3.58953414856893
H	9.34316644767724	-1.74883759785844	3.98416004606626
C	9.14056640985280	0.38087752333028	4.37916425170610
H	9.55984498996226	0.30612961457771	5.39409468023297
C	8.72499727635851	1.62796245135710	3.88875439988857
H	8.81414063372629	2.52704501204435	4.51772239979059
C	8.18337504413211	1.74657909469587	2.59521170495784
C	2.02022870784718	-3.41157718151232	-0.26697823107327
H	1.84914386234490	-2.73391843697579	-1.13161399272398
H	3.09482794857334	-3.68641743662844	-0.29762303091665
H	1.41622598947571	-4.32591428254753	-0.42891141759331
C	2.43939280044979	0.34921935192662	3.23131418399430
H	1.80352785142242	0.76418810157621	4.03735034869034
H	3.46266288734459	0.21952794099255	3.64127248272070
H	2.51512290903241	1.10675079477859	2.42354770988028
C	5.36899979234741	-1.71494387174047	-2.78552562271402
H	6.45695013613668	-1.59057584522142	-2.96332141084567
H	5.23963982150511	-2.13974987000132	-1.76604233202647
H	4.98089119999446	-2.44627087663942	-3.51907413269358
C	8.31337984968222	-1.92084480904544	1.42218308102631
H	7.23347930269776	-2.09940222276740	1.22919778901542
H	8.80521805318934	-1.79437354347500	0.43542879064364
H	8.73469979878033	-2.82175056970983	1.90610399184185
C	7.70215343575137	3.06202139609528	2.03934658291343
H	8.28609121363352	3.36231089269628	1.14402105134984
H	6.63847848022785	2.99010052779961	1.72946416011216
H	7.79000814127874	3.86927565079293	2.79038716041214
C	4.68597631962466	3.01057061199343	-1.10139188798676
H	4.47635171940527	2.70257143065953	-0.05296528030077
H	5.77019637083909	3.24073783132985	-1.16017021798059
H	4.11993971497959	3.93752347135478	-1.30903087881099

4:

Cl	10.10919157304687	14.30516198854070	7.71008748374390
Cl	8.29669643197445	16.71817426071651	5.82313494578604
Cl	23.77400451223333	9.98689887115837	1.24694731855184
Cl	24.80788232713544	7.45359144133575	3.54651928796482
P	13.38074860997578	16.60357962949245	3.74760320833973
P	14.30666034407592	14.61222848157993	3.68142180968212
P	16.25912118060964	14.64110261900017	4.88018278884008

P	17.35540293601989	13.29992751743305	3.39815682657703
P	16.02716575401535	12.41224784765098	4.94751424747926
P	18.27841877482010	12.34466936882164	5.22661718336223
P	18.55842265376612	10.37155591654463	4.11068692425295
P	19.99211336171989	9.27937382073455	5.37966129009260
N	11.91207644019719	15.18853519846624	5.84153822600186
N	10.78198750572459	16.70663680568246	4.70361516518988
N	21.73059702473203	9.83948333694300	3.06033882383019
N	22.38770707678471	8.28482785449419	4.48016654107312
C	12.02654535198334	16.09775965020456	4.79440765260639
C	12.98258872630997	14.50843840236928	6.52661361581869
C	13.04521746096342	13.09624418550843	6.46584135887416
C	14.01364846156154	12.45332556321555	7.26062977226639
H	14.09336756072582	11.35696025638471	7.21263193102603
C	14.89291939649073	13.19206271479007	8.06680129459419
H	15.65882210600407	12.67189882189734	8.66083105982116
C	14.82196626499951	14.59048547796003	8.08860497993705
H	15.52594198480060	15.16991297885619	8.70474613845721
C	13.85001329837014	15.28069511145344	7.33773303091506
C	10.60884718090697	15.24154272993157	6.37326002501368
C	9.91340035858043	16.19110254265786	5.66911678621724
C	10.41356200835794	17.62890306240907	3.66622861778758
C	10.41931329856443	19.00890098737110	3.96196407963428
C	10.03751131564434	19.89216454978669	2.93476087454622
H	10.03516469109295	20.97524077586819	3.13218996356603
C	9.67385613398272	19.40475414275204	1.67037219219532
H	9.38007049134551	20.10968241630014	0.87767162875866
C	9.68764055757818	18.02686387879585	1.40584605162390
H	9.40918814918077	17.65248150407090	0.40875285100354
C	10.05834117620906	17.10535419516627	2.40276232122372
C	15.01174714319846	14.50580201751087	1.95821370022342
C	15.89772787523799	15.46965320005233	1.39262647472297
C	16.5135577869328	15.18831863583682	0.15730326897307
H	17.20212537349801	15.93150999698675	-0.27566970330971
C	16.26945063288513	13.98414923078086	-0.51782262454411
H	16.76779408812730	13.77783432727854	-1.47783362038745
C	15.38582177916102	13.04835005037068	0.03145033618140
H	15.18956333764644	12.10102533094176	-0.49504502800949
C	14.74370505271187	13.28850794606342	1.26417840344936
C	16.89420858739522	9.59946710249840	4.45805736862691
C	16.38246536715859	9.29227382470565	5.75418616670932
C	15.04815336066059	8.85724358175719	5.87637254651962
H	14.65606435204691	8.62034822084379	6.87858365124950
C	14.21835765045536	8.73070270889892	4.75365969544533
H	13.17655425300581	8.39394420558481	4.87027044517647
C	14.72213642308947	9.03395939792306	3.48392921382263
H	14.07307217810872	8.94257668646639	2.59911631058681
C	16.05237492992777	9.47143303139291	3.31195908714105
C	21.34620354993527	9.17339405496476	4.22062482774086
C	21.06414772727803	10.94863321355264	2.43385011839363
C	21.18643798567238	12.22508822189189	3.02510283353434
C	20.51981178598382	13.29251371051519	2.39380552106387
H	20.56918169857169	14.29435971727607	2.84634247315836
C	19.77554048676646	13.08533449836739	1.22329475696128
H	19.23263716100944	13.92393531642692	0.76283289179870
C	19.68910870745787	11.80620034747799	0.65224327527449
H	19.08114368056627	11.64887993905471	-0.25159767550086
C	20.33695928957180	10.71101573097535	1.24621130067276
C	22.98281014522587	9.36526214622632	2.62649280222178
C	23.39019600974655	8.40469217995921	3.51441064232416
C	22.39127734579905	7.34615334034598	5.56552347705324
C	21.72578927418805	6.11313186638319	5.38713667058943
C	21.75015207461430	5.20570038442545	6.46247352797237
H	21.23829937285553	4.23670575929763	6.35710509494459
C	22.41234854049921	5.52690541727302	7.65717891525011
H	22.42098047367844	4.80413795834631	8.48739830031386
C	23.05813073915028	6.76371436806894	7.80523534413075
H	23.56654173836008	7.01306605306957	8.7493768514356
C	23.05769697278445	7.70340162993806	6.75750761010820
C	10.12787954116914	15.62469457591065	2.14405996366089
H	9.58891747358291	15.04541277678261	2.92173981804356
H	9.70063978196556	15.36767439321996	1.15669708576492
H	11.19053014674353	15.29492986649153	2.16896145851397
C	10.84379106791664	19.49411836475552	5.32471978805698
H	10.13740283452049	19.15836998780067	6.11282910934692
H	11.84502062891261	19.09544780189510	5.58959384366673
H	10.89074262019669	20.59888640800471	5.35805551499351
C	12.14839113039905	12.31080019114051	5.54739528170533

H	11.13764976856286	12.16582598214089	5.98479538573029
H	12.03495424814579	12.84081922074623	4.58106157954207
H	12.58548491688203	11.31429203181344	5.34262724562613
C	13.75098759856121	16.78008015935369	7.37381977134310
H	14.07103551062784	17.20792632241202	6.39553494797757
H	12.70664874004430	17.11825038021590	7.53867192654796
H	14.38649727548382	17.20294289677429	8.17427367540329
C	16.21344779587602	16.76921014837893	2.08639147013974
H	16.50253474800421	16.60508172737175	3.14631946086127
H	17.04132821348140	17.30258717455670	1.58066029037110
H	15.32984484438053	17.44189956747066	2.10220789838729
C	13.82367645567129	12.22933410332017	1.82495092509893
H	12.84242141084937	12.65213451446827	2.12011730261204
H	13.65286260128414	11.42761788149492	1.07988938051816
H	14.25057690644590	11.76764998274503	2.74020704089691
C	16.52408198955219	9.83575248593690	1.92231586106533
H	16.71989981971812	10.92573795887913	1.83514159398954
H	17.47675745499101	9.33215473554691	1.66675607578587
H	15.76250573001620	9.56035919505815	2.16640908414053
C	17.20663335776850	9.45747102302966	7.00417769067045
H	16.58101148894642	9.35252922189794	7.91169560865844
H	18.02063068899454	8.70419414115711	7.05583147647033
H	17.69859376016111	10.45305783616948	7.03368456351519
C	20.20039180405706	9.31046295604358	0.71295150456612
H	21.17779904245831	8.89261278197149	0.39331920357291
H	19.80004032880795	8.63855753574089	1.50226413978217
H	19.51476005962648	9.27730022820501	-0.15457401059675
C	20.98970476301620	5.82620224201988	4.10596823905731
H	20.12766331422751	6.52265980677024	4.00796753008407
H	21.63720885296595	5.97990965037844	3.21825001433624
H	20.60788254858801	4.78820855371489	4.08436673009591
C	23.71282537599152	9.05445197824605	6.88356611488194
H	24.54484833519378	9.17117847709149	6.15768792397207
H	22.97981697887676	9.86261200521449	6.67804766212522
H	24.12236887736399	9.20690302459550	7.89985198846308
C	21.94514883547201	12.40498245005911	4.31213228596530
H	21.40578880609111	11.90381295900812	5.14772652530994
H	22.95438678763950	11.94627673758796	4.26096950999440
H	22.05480765123017	13.47578810033724	4.56567663690411

P₄:

P	2.85914638604243	7.55272601418640	26.38289204704455
P	2.49943940854460	8.58433727984623	24.43725668079501
P	0.77518733810494	8.02128768351791	25.73698208828669
P	2.14812686730802	9.66774902244945	26.35616928387375

5 Crystallography

5.1 General Remarks

Suitable single crystals were coated with Paratone-N oil or Fomblin Y25 PFPE oil, mounted using a glass fiber and frozen in the cold nitrogen stream. X-ray diffraction data were collected at 100 K on a Rigaku Oxford Diffraction SuperNova diffractometer using either Cu K α radiation ($\lambda = 1.54184 \text{ \AA}$) generated by micro-focus sources. The data reduction and absorption correction was performed using CrysAlisPro¹³, respectively. Using Olex2¹⁴, the structures were solved with SHELXT¹⁵ by direct methods and refined with SHELXL¹⁶ by least-square minimization against F^2 using first isotropic and later anisotropic thermal parameters for all non-hydrogen atoms. Hydrogen atoms were added to the structure models on calculated positions using the riding model. Images of the structures were produced with the Olex2¹³ software.

5.2 Crystallographic data

Table S5: Crystallographic Data for selected structures.

Compound	1	4	5
Empirical formula	C ₃₉ H ₅₁ Cl ₂ N ₂ P ₂	C ₈₄ H ₁₀₇ Cl ₄ FN ₄ P ₈	C ₈₈ H ₁₂₆ Cl ₄ N ₄ O ₂ P ₄
Formula weight [g/mol]	680.66	1581.29	1537.60
Temperature [K]	99.96(12)	100.00(10)	100.01(10)
Crystal system	triclinic	monoclinic	monoclinic
Space group	P-1	P2 ₁ /c	C2/c
a [Å]	10.8940(3)	22.39630(10)	14.63850(10)
b [Å]	11.6371(3)	24.84720(10)	34.7552(3)
c [Å]	17.3041(2)	15.60040(10)	18.1897(2)
a [°]	86.498(2)	90	90
β [°]	73.235(2)	96.9330(10)	109.1670(10)
γ [°]	66.584(2)	90	90
Volume [Å ³]	1923.91(8)	8617.92(8)	8741.26(14)
Z	2	4	4
ρ _{calc} [g/cm ³]	1.175	1.219	1.168
μ [mm ⁻¹]	2.508	3.008	2.278
F(000)	726.0	3344.0	3304.0
Crystal size [mm ³]	0.545 × 0.441 × 0.377	0.2 × 0.15 × 0.03	0.16 × 0.08 × 0.06
Radiation (λ in Å)	Cu Kα (λ = 1.54184)	Cu Kα (λ = 1.54184)	Cu Kα (λ = 1.54184)
2θ range for data collection [°]	5.344 to 154.58	5.334 to 153.744	5.086 to 153.594
Index ranges	-13 ≤ h ≤ 13, -13 ≤ k ≤ 14, -21 ≤ l ≤ 21	-28 ≤ h ≤ 23, -31 ≤ k ≤ 28, -19 ≤ l ≤ 19	-16 ≤ h ≤ 18, -43 ≤ k ≤ 43, -22 ≤ l ≤ 22
Reflections collected	21226	89080	53294
Independent reflections	8000 [R _{int} = 0.0228, R _{sigma} = 0.0203]	18007 [R _{int} = 0.0386, R _{sigma} = 0.0280]	9164 [R _{int} = 0.0396, R _{sigma} = 0.0263]
Data/restraints/parameters	8000/0/418	18007/547/1030	9164/90/499
Goodness-of-fit on F ²	1.053	1.022	1.041
Final R indexes (I ≥ 2σ(I))	R ₁ = 0.0421, wR ₂ = 0.1139	R ₁ = 0.0474, wR ₂ = 0.1241	R ₁ = 0.0415, wR ₂ = 0.0930
Final R indexes (all data)	R ₁ = 0.0426, wR ₂ = 0.1143	R ₁ = 0.0542, wR ₂ = 0.1290	R ₁ = 0.0455, wR ₂ = 0.0954
Largest diff. peak/hole [e/Å ³]	0.68/-0.30	0.82/-0.83	0.31/-0.73
CCDC Number	2351433	2351435	2351434

- 1 M. H. Holthausen, S. K. Surmiak, P. Jerabek, G. Frenking and J. J. Weigand, *Angew. Chem. Int. Ed.*, 2013, **52**, 11078–11082.
- 2 K. Schwedtmann, F. Hennersdorf, A. Bauzá, A. Frontera, R. Fischer and J. J. Weigand, *Angewandte Chemie*, 2017, **129**, 6314–6318.
- 3 K. Schwedtmann, J. Haberstroh, S. Roediger, A. Bauzá, A. Frontera, F. Hennersdorf and J. J. Weigand, *Chem. Sci.*, 2019, **10**, 6868–6875.
- 4 L. R. Smith and J. L. Mills, *J. Am. Chem. Soc.*, 1976, **98**, 3852–3857.
- 5 N. G. Connelly and W. E. Geiger, *Chem. Rev.*, 1996, **96**, 877–910.
- 6 J. M. Savéant and C. Costentin, *Elements of molecular and biomolecular electrochemistry. An electrochemical approach to electron transfer chemistry*, Wiley, Hoboken, NJ, 2019.
- 7 R. Ahlrichs, M. Bär, M. Häser, H. Horn and C. Kölmel, *Chem. Phys. Lett.*, 1989, **162**, 165–169.
- 8 a) A. D. Becke, *J. Chem. Phys.*, 1996, **104**, 1040–1046; b) J. P. Perdew, *Phys. Rev. B*, 1986, **33**, 8822–8824;
- 9 S. Grimme, J. Antony, S. Ehrlich and H. Krieg, *J. Chem. Phys.*, 2010, **132**, 154104.
- 10 A. Klamt, *WIREs Comput Mol Sci*, 2011, **1**, 699–709.
- 11 K. B. Wiberg, *Tetrahedron*, 1968, **24**, 1083–1096.
- 12 E. D. Glendening, J. K. Badenhoop, A. E. Reed, J. E. Carpenter, J. A. Bohmann, C. M. Morales, P. Karafiloglou, C. R. Landis, F. Weinhold, *NBO 7.0*, accessed 28 November 2023.
- 13 *CrysAlisPRO*, Oxford Diffraction / Agilent Technologies UK Ltd.
- 14 O. V. Dolomanov, L. J. Bourhis, R. J. Gildea, J. A. K. Howard and H. Puschmann, *J. Appl. Cryst. (Journal of Applied Crystallography)*, 2009, **42**, 339–341.
- 15 G. M. Sheldrick, *Acta Cryst.*, 2015, **A71**, 3–8.
- 16 G. M. Sheldrick, *Acta Cryst.*, 2015, **C71**, 3–8.